Proceedings of Global Power and Propulsion Society
ISSN-Nr: 2504-4400
GPPS Hong Kong 2023
October 17-19, 2023
www.gpps.global

# GPPS-TC-2023-0167

# A Mean-Fluctuation Decomposition Scheme to Accelerate the Simulation of Unsteady Conjugate Heat Transfer

**Feixue Cai**
**Tsinghua University**
caifx22@tsinghua.edu.cn
Beijing, China

**Hua Zhou**
**Tsinghua University**
zhouhua@tsinghua.edu.cn
Beijing, China

**Min Yao**
**Tsinghua University**
minyao@tsinghua.edu.cn
Beijing, China

**Zhuyin Ren**
**Tsinghua University**
zhuyinren@tsinghua.edu.cn
Beijing, China

## ABSTRACT

The unsteady conjugate heat transfer simulation technology has to address both the computational cost and the stiffness issues originated from the wide disparate time scales between the fluid and solid domains, especially in the combustion chamber. Although the existing desynchronizing coupling model can significantly improve the computational efficiency, this model always amplifies the fluctuation amplitudes of the fluid-solid interface temperature. To tackle this issue of losing solution accuracy occurred in the desynchronized model, a mean-fluctuation decomposition scheme is adopted in the present study, and a novel fluid-solid-solid solver coupling procedure is further proposed for the simulations of combustor liner with thermal barrier coating. Finally, the decomposition scheme and the proposed coupling procedures are validated in a simplified one-dimensional test of the combustor, including the solid liner-fluid and solid liner-TBC-fluid cases. The test results demonstrate that the computation acceleration is significantly enhanced by the mean-fluctuation decomposition model while the solution accuracy is also ensured for the solid-liner-fluid coupling case. For the solid liner-TBC-fluid coupling case, the designed fluid-solid-solid coupling procedure accurately predicts the evolution of each interface temperature after employing the TBC, which also achieves a certain acceleration compared to the conventional synchronizing coupling model.

## INTRODUCTION

Nowadays, propulsion and power-generation systems are encountering local overheating and increasing risk of thermal fatigue cracks due to the extreme operating conditions (Lv et al., 2010; Zhang et al., 2020), especially the combustor. The accurate life assessment of the combustor liner and the Thermal Barrier Coating (TBC) materials mainly rely on the reliable prediction of the heat transfer near the walls of a combustion chamber. In practice, the heat transfer at the fluid-solid interface can be caused by the system's transient start or the different operating transitions, and also occurs because of the turbulent reacting flow field. Thus, Conjugate Heat Transfer (CHT) process is inevitably transient. Although unsteady CHT is better for engineering applicability, the stiffness issue of wide disparity of time scales has to be addressed. For the numerical scheme's stability requirement, the fluid solver's time step size is usually several orders of magnitude smaller than that of the solid solver, and the fluid time step $\Delta t_f$ and solid time step $\Delta t_s$ gives a ratio of $\Delta t_s/\Delta t_f \approx 10{,}000$ (He and Oldfield, 2010). To maintain the physical time consistency, it will cost over millions of time step. This multi-scale property is the main challenge in the study of unsteady CHT.

In order to predict the unsteady CHT process, a fully coupled approach is proposed (Birken et al., 2010; Geiser and Güttel, 2012; Lindström and Nordström, 2010). it integrates the entire set of governing equations of the fluid and solid domain as a single system, which means not physically distinguish between the fluid and solid but mathematically solve them. Fully coupled approach maintains high computational accuracy but limited application range since it requires that both the fluid and solid fields are solved by the same numerical approach under the unified framework. In contrast, a loosely coupled approach is proposed, which is to interact different solvers and achieve coupling through variable passing. The

loosely coupled approach allows each solver works independently, and the continuity of temperature and heat flux can be obtained after an iterative procedure (Verstraete and Van den Braembussche, 2009). The loosely coupled approach can significantly improve the computational efficiency, and is more applicable for engineering problems.

Based on loosely coupled approach, a fully decoupling model was proposed in the late 1990s (Li and Kassab, 1994; Giles, 1997; Heselhaus and Vogel, 1995). It solves the solid domain as a steady state since the characteristic time of heat transfer in the fluid domain is much smaller than that in the solid domain. Also, a similar way which treats the fluid domain as a quasi-steady state is proposed (Errera and Chemin, 2013; Errera and Baqué, 2013; Errera et al., 2020; Errera et al., 2017; Baqué et al., 2013; Gimenez et al., 2016). However, the fully decoupling model can hardly be applied in the simulation of the combustor near-wall heat transfer combined with Large Eddy Simulation (LES) or Direct Numerical Simulation (DNS) since it cannot reflect the transient response at the solid end in time. Thus, a desynchronizing model was proposed for the efficient thermal simulation of combustion using high-fidelity codes. For example, Duchaine et al. (Duchaine et al., 2009b; Duchaine et al., 2009a) introduced this coupling strategy in which the codes are advanced at the same convergence rate by accelerating the thermal solver. The desynchronizing model consists of computing the unsteady fields in both fluid and solid mediums while desynchronizing them, which means that each unsteady solver works with its own time step independently and then couples after a specific physical time interval. It was lately applied and validated by Duchaine et al. (Duchaine et al., 2014; Duchaine et al., 2015), Jauré et al. (Jauré, 2012; Jaure et al., 2013) and Berger et al. (Berger et al., 2016). For the desynchronizing model, the physical time interval of fluid-solid coupling is defined as coupling time step $\Delta t_{cpl}$, and the solid solver's time step is usually set as the same as the coupling time step. The specific value of the time step ratio between the coupling time step and the fluid solver's time step is called the desynchronization factor $\alpha$, which is expressed as $\alpha = \Delta t_{cpl}/\Delta t_f$. However, the solid's time step is larger than the fluid's time step, which means that the heat flow frequency seen in the solid domain is lower than the real frequency seen in the fluid domain. If the frequency seen in the solid domain is greatly attenuated (the solid's time step is often scaled up to 10-1000 times the fluid's time step in simulations), this will cause a problem: over-prediction of the fluctuation amplitude (Koren et al., 2017a). Therefore, it is necessary to further develop coupling procedure that guarantee both the accuracy and efficiency, and can be applied to different cases such as fluid-solid and fluid-solid-solid coupling.

The present study will focus on developing and investigating the appropriate coupling strategy for fluid-solid and fluid-solid-solid coupling applications. In Section 2, a hybrid-cell interface model for the fluid-solid interface is firstly described, and the mean-fluctuating decomposition scheme is introduced and applied. Furthermore, a coupling procedure is developed to increase the computational efficiency for fluid-solid-solid coupling. The test cases for the calculation of the near-wall heat transfer simplified from real engine combustor conditions is introduced in Section 3, and then these coupling strategies are validated under fluid-solid and fluid-solid-solid coupling cases. Finally, the conclusion will be presented in Section 4.

## METHODOLOGY

### Hybrid-cell interface model

For a control volume of fluid domain, the continuity equation for mass conservation is

$$\frac{\partial \rho}{\partial t} + \boldsymbol{\nabla} \cdot (\rho \boldsymbol{u}) = 0 \tag{1}$$

where $\rho$ represents the density and $\boldsymbol{u}$ is the velocity. For incompressible flow, representing pressure with $p$, dynamic viscosity with $\mu$ and body force with $\boldsymbol{f}$, the momentum equation can be written as

$$\rho \frac{\partial \boldsymbol{u}}{\partial t} + \rho(\boldsymbol{\nabla} \cdot \boldsymbol{u})\boldsymbol{u} = -\boldsymbol{\nabla} p + \mu \boldsymbol{\nabla}^2 \boldsymbol{u} + \boldsymbol{f} \tag{2}$$

The heat transfer equation for a fluid domain without radiation term is

$$\rho_f c_{p,f} \frac{\partial T_f}{\partial t} + \rho_f c_{p,f} \boldsymbol{u} \cdot \boldsymbol{\nabla}(T_f) = \boldsymbol{\nabla} \cdot (\lambda_f \boldsymbol{\nabla} T_f) \tag{3}$$

where the subscript $f$ represents the fluid, $c_p$ is the heat capacity and $\lambda$ is the thermal conductivity. For a solid domain, there is no convection term, thus the heat transfer equation for the solid is

$$\rho_s c_{p,s} \frac{\partial T_s}{\partial t} = \boldsymbol{\nabla} \cdot (\lambda_s \boldsymbol{\nabla} T_s) \tag{4}$$

where the subscript $s$ represents the solid.

Unsteady conjugate heat transfer is normally carried out by running two different simulation codes for both domain and the two domains share the common interface where both codes need to be coupled, thus this common interface must maintain the continuity of the temperature and heat flux. The standard Neumann-Dirichlet boundary approach is commonly used to yield algebraic coupling equations (Verstraete and Van den Braembussche, 2009), which means that one solver

provides a fixed temperature as the Dirichlet boundary at the interface while the other one uses Neumann condition with a given heat flux. However, Neumann-Dirichlet boundary does not allow a direct way to define an error indicator and adapt the coupling time step. For the hybrid-cell coupling model proposed by Koren et al. (Koren et al., 2017b), it can obtain the interface temperature independently and give the other solver a Dirichlet boundary condition.

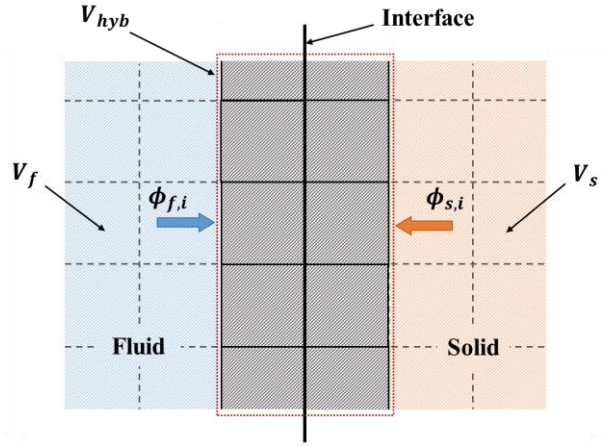


**Figure 1 Schematic plot of hybrid cells**

The hybrid-cell interface model relies on the energy coupling for the interface cells between the fluid and solid domains. As shown in Figure 1, for the conformal meshes, the hybrid cell $V_{hyb}$ is composed of the fluid and solid mesh cells, $V_f$ and $V_s$, respectively, on each side of the fluid-solid interface. For the hybrid cell $V_{hyb}$, its enthalpy $H_{hyb}$ evolves according to the following,

$$\frac{dH_{hyb}}{dt} = -\phi_{s,i} - \phi_{f,i} \tag{5}$$

where $\phi_{s,i}$ is the heat flux integrated over all internal faces in the solid domain and $\phi_{f,i}$ is that in the fluid domain. The first order approximation can be made by assuming the temperature inside the hybrid cell is equal to interface temperature $T_i$, the evolution of $H_{hyb}$ can be split into the solid and fluid contributions,

$$\frac{dH_{hyb}}{dt} = \int_{V_f} \rho_f c_{p,f} \frac{dT_i}{dt} dV + \int_{V_s} \rho_s c_{p,s} \frac{dT_i}{dt} dV \tag{6}$$

With the variations of thermo-physical properties in each cell being neglected, the above equation can be simplified as

$$\frac{dH_{hyb}}{dt} = \left(V_f \rho_f c_{p,f} + V_s \rho_s c_{p,s}\right) \frac{dT_i}{dt} \tag{7}$$

Hence, the temporal evolution of interface temperature is governed by the following ordinary differential equation (ODE)

$$\frac{dT_i}{dt} = -\frac{\phi_{f,i} + \phi_{s,i}}{\rho_f c_{p,f} V_f + \rho_s c_{p,s} V_s} \tag{8}$$

During a coupling time step ($\Delta t_{cpl}$), each solver does their own iterations independently. The three time steps are related by $\Delta t_{cpl} = N_s \Delta t_s = N_f \Delta t_f$, where $N_f$ and $N_s$ are the numbers of iterations for fluid and solid solvers, respectively. The coupling procedure starts at a time $t^n$, and then each solver integrates to the next time step $t^{n+1}$ independently. After every integration step, the heat flux $\phi_{s,i}^{n+1}$ and $\phi_{f,i}^{n+1}$ are updated, and then the Eq. (8) is solved to update the interface temperature $T_i^{n+1}$. Between $t^n$ and $t^{n+1}$, the iterations produce a group of discrete values, like $\phi_{f,i}^p$ and $\phi_{s,i}^q$ corresponding to the solvers' inner steps $\Delta t_f^p$ and $\Delta t_s^q$. Thus, the heat flux from the fluid side (a similar way in solid side) between the two coupling steps is the time averaged and face-integrated flux

$$\hat{\phi}_{f,i} = \frac{1}{\Delta t_{cpl}} \sum_{p=1}^{N_f} \phi_{f,i}^p \Delta t_f^p \tag{9}$$

Hence, the Eq. (8) can be written as

$$T_i^{n+1} = T_i^n - \Delta t_{cpl} \frac{\hat{\phi}_{f,i} + \hat{\phi}_{s,i}}{\rho_f c_{p,f} V_f + \rho_s c_{p,s} V_s} \tag{10}$$

### Mean-fluctuation decomposition scheme

In the process of CHT, the convergence rate of the solid domain is orders of magnitudes slower than that of the fluid domain. For the conventional desynchronized coupling of unsteady fluid and solid solvers, the accuracy of heat transfer is limited by the desynchronized factor of fluid (solid) time steps. Considering the heat in the wall is linearly transferred, the solution can be divided into steady state and unsteady state (Koren et al., 2017a). Namely that the linear heat conduction equation of solid enables one to decompose the solid temperature into the mean and fluctuation part,

$$T_s = \hat{T}_s + T_s' \tag{11}$$

The time mean temperature $\hat{T}_s$ is solved by steady-state heat conduction equation while the fluctuating temperature $T_s'$ is solved by the unsteady one

$$0 = \boldsymbol{\nabla} \cdot \left(\lambda_s \boldsymbol{\nabla} \hat{T}_s\right) \tag{12}$$

$$\rho_s c_{p,s} \frac{\partial T_s'}{\partial t} = \boldsymbol{\nabla} \cdot (\lambda_s \boldsymbol{\nabla} T_s') \tag{13}$$

For solving Eq. (12), a steady-state heat conduction solver is needed. In this solver, the boundary condition at the interface is the statistical steady-state value of heat flux, e.g., the time mean value

$$\hat{\phi}_i(\tau) = \frac{1}{\tau}\int_0^{\tau} \phi_i(t)dt \tag{14}$$

$$\phi_i' = \phi_i - \hat{\phi}_i \tag{15}$$

Also, the interface temperature is divided in to mean and fluctuating parts $T_i = \hat{T}_i + T_i'$. The hybrid-cell equation for the fluctuating term now becomes

$$\frac{dT_i'}{dt} = -\frac{\phi_{f,i}' + \phi_{s,i}'}{\rho_f c_{p,f} V_f + \rho_s c_{p,s} V_s} \tag{16}$$

Note that $\hat{\phi}_i(\tau)$ is determined by the total computational time $\tau$, which means that the steady-state heat conduction solver is actually time dependent. However, $\hat{\phi}_i(\tau)$ will gradually move to a statistically stable state, and $\hat{T}(\tau)$ will change accordingly. Once the average interface heat flux converges, the average solid temperature field converges, and it thus achieves the computing acceleration.

### Coupling procedure for solid liner-TBC-fluid system

For the TBC related problems, the evolution of wall temperature will be very important information, especially in the areo-engine combustor liners. As mentioned above, the characteristic time of solid's heat conduction is much larger than that of fluid's heat transfer, and because the TBC material itself has a low thermal conductivity (0.1~0.01 of the liner's) (Song et al., 2023), this gap will be even greater in solid liner-TBC-fluid system. In order to achieve the acceleration, a coupling procedure based on the hybrid-cell interface model and mean-fluctuation decomposition scheme is proposed and shown in Figure 2.

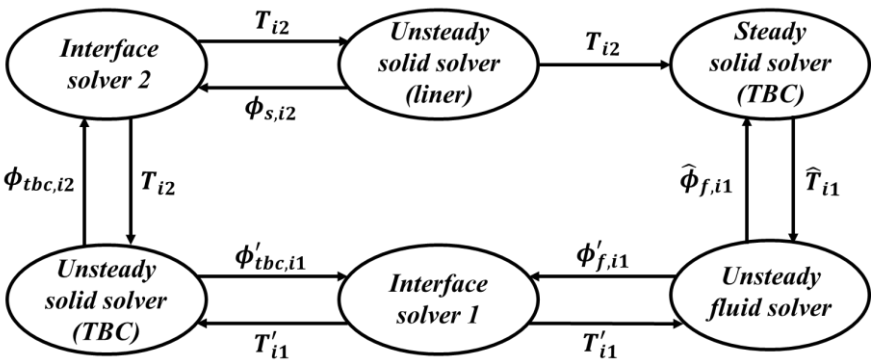


**Figure 2 Coupling procedure for solid liner-TBC-fluid system**

The subscript '1' represents the TBC-fluid interface while '2' represents the liner-TBC interface. In this procedure, the boundary conditions of this system are applied to the liner's unsteady solid solver and the unsteady fluid solver. For the TBC-fluid interface, the mean-fluctuation decomposition scheme is adopted for acceleration; For liner-TBC interface, a direct hybrid-cell interface model is employed considering that the convergence characteristics of solid liner and TBC

are similar. Therefore, the overall coupling procedure is as follows: A series of initial conditions are given at $t^0 = 0$, in which the fluctuating terms are all zero; At $n$ time step, the interface temperature $T_{i1}^{n+1} = T_{i1}'^{n+1} + \hat{T}_{i1}^{n+1}$ is calculated by the interface solver '1' and steady solid solver (TBC), and the interface temperature $T_{i2}^{n+1}$ is calculated by interface solver '2'; The unsteady temperature fields of TBC and fluid for next step are updated; The interface's heat flux including $\phi_{tbc,i2}^{n+1}$, $\phi_{tbc,i1}'^{n+1}$, $\phi_{f,i1}'^{n+1}$ and $\hat{\phi}_{f,i1}^{n+1}$ are calculated based on the temperature fields, and these variables are applied to the $(n+1)$ time step.

Different from the synchronizing procedure, this procedure with mean-fluctuation decomposition scheme can accelerate the convergence owing to the fast calculations of the steady-state terms. In fact, this is a feasible and effective method in the engineering applications, because the steady-state calculation is usually adopted to advance to the near statistical steady-state in the large high-fidelity engine simulations, and then the unsteady state calculation is carried out to obtain the unsteady characteristics of temperature field, such as temperature fluctuation at the interface. This procedure advances the steady-state solver and unsteady-state solver synchronously, which is equivalent to automating the above hybrid cell model and mean-fluctuation decomposition scheme in order to accelerate the unsteady CHT computations.

## RESULTS AND DISCUSSION

### Configuration of test cases

According to the above described models and schemes for the unsteady CHT calculations, a 1-D solid liner-fluid heat transfer and a 1-D solid liner-TBC-fluid heat transfer test cases were established to validate the methods, as shown in Figure 3(a) and Figure 3(b), respectively.

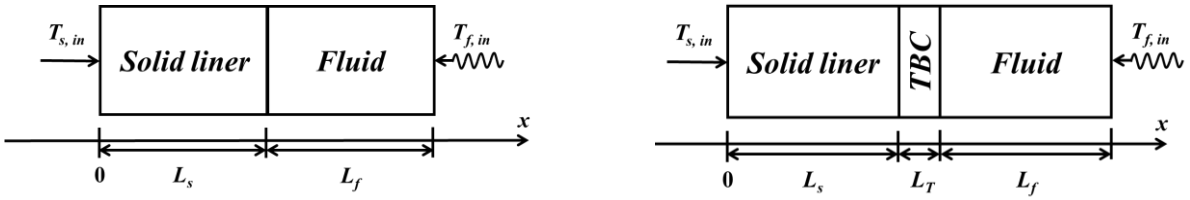


(a) Case 1 (b) Case 2

**Figure 3 Configurations of (a) Case 1: solid liner-fluid, and (b) Case 2: solid liner-TBC-fluid**

The left edge of the solid liner is located at $x = 0$, and the length of the solid liner and the fluid domains is $L_s = 10$ mm and $L_f = 1$ mm, respectively. Given that the thickness of the TBC is usually orders of magnitude smaller than that of the solid liner, it is chosen here as $L_T = 0.5$ mm. The boundary conditions at both domain edges are set as follows. For the left side of the solid domain, a constant temperature boundary condition taken from the cooling flow is considered, where the temperature is $T_{s,in} = 800$ K under the real gas turbine conditions. For the right side of the fluid domain, a sinusoidal temperature input $T_{f,in} = 1200 + 800\sin(2\pi f_{re} t)$ is considered to represent the heat loads caused by the hot turbulent swirling flow in the combustor, where the frequency $f_{re} = 1$ Hz for the solid liner-fluid test case and $f_{re} = 100$ Hz for the solid liner-TBC-fluid test case.

The 1st order implicit Euler scheme is applied to the discretization of the time partial derivation, while the central difference scheme is applied to the displacement. The material of solid is an Inconel steel, and the fluid is the burnt gases of oxy-combustion. As for the TBC, it is ceramic only and is made of Yttria-Stabilized Zirconia (YSZ), a material commonly used for thermal barrier coatings on aeroengines (Liu et al., 2019). The thermal physical properties and iterative parameters of all three mediums for different cases are listed in Table 1. It should be noted that in the present test cases, the fluid and solid's thermal conductivities are artificially changed to reduce the ratio of fluid-solid heat transfer time scale, so that the accurate numerical solution can be obtained with less computational cost.

**Table 1 Thermal physical properties of the solid liner, TBC and fluid mediums**

| Properties/Parameters | Case 1 | | Case 2 | | |
|---|---|---|---|---|---|
| | Solid liner | Fluid | Solid liner | TBC | Fluid |
| $\rho$ $(\mathrm{kg/m^3})$ | 8510 | 3.65 | 8510 | 2000 | 3.65 |
| $C_p$ $(\mathrm{J/kg \cdot K})$ | 439 | 1738 | 439 | 600 | 1738 |
| $\lambda$ $(\mathrm{W/m \cdot K})$ | 117 | 0.0158 | 117 | 2 | 0.158 |
| $\Delta x$ (mm) | $10^{-2}$ | $10^{-1}$ | $2\times10^{-2}$ | $10^{-2}$ | $10^{-1}$ |
| $\Delta t$ (s) | $10^{-4}$ | | $10^{-5}$ | | |

### Performance with mean-fluctuation decomposition scheme

In order to validate the acceleration effect of mean-fluctuation decomposition scheme, a series of simulations based on Case 1 settings are carried out. Figure 4 shows the evolution of temperature at the solid liner-fluid interface $T_i$ predicted by different coupling schemes over fluctuating periods $N_P$ (computational time for one period is $1/f_{re}$).

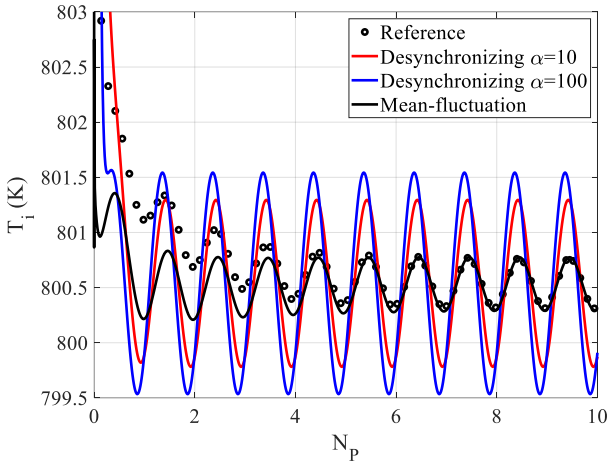


**Figure 4 Comparison of solid liner-fluid temperature evolutions using different coupling schemes**

For Case 1, the synchronizing scheme can be used to obtain accurate numerical solutions. However, the convergence of this scheme is slow, as shown by the black dotted line in Figure 4, where the reference solution is the results based on the synchronizing scheme. It takes about 6 periods to reach steady state in this synchronizing scheme, while the desynchronizing model can accelerate the convergence despite overestimating the temperature fluctuation. The red and blue solid lines represent the predicted results with the desynchronization factor $\alpha$=10 and 100, respectively. It can be observed that both results reach the steady state at approximately one period, but the fluctuation amplitudes are overestimated about 200% and 300% at $\alpha$=10 and 100, respectively. In contrast, the prediction results of mean-fluctuation decomposition scheme can reach the steady state faster and predict the fluctuation accurately, as shown by the black solid line in Figure 4. The steady state can be reached at about one period by adopting this decomposition scheme, and the relative error of prediction of fluctuation quantity is less than $3.25\times10^{-3}$%. However, at the same time, it should be noted that the mean-fluctuation decomposition method could not alleviate the numerical oscillation in the early prediction stage. Note that in this test case, in order to obtain an accurate numerical solution with a small computational cost, the ratio of fluid-solid heat transfer time scale is artificially reduced to about 8. Consequently, the acceleration ratio is about 6 times by using the mean-fluctuation decomposition scheme. Considering the real thermal conductivity of fluid and solid, the ratio of time scale of fluid-solid heat transfer can be up to 100 times. Therefore, it can be expected that for practical problems, the6celeration ratio obtained by the mean-fluctuation decomposition method will be more than 10 times or even larger.

### Performance with solid liner-TBC-fluid coupling procedure

The TBC technology is usually to attach materials with high temperature resistance, corrosion resistance and low thermal conductivity to the surface of metal components in the form of coating, so as to reduce the temperature borne by materials and improve the stability and service life of metal components (Song et al., 2023). In the design of TBC, the evolution of wall temperature (which is also the interface temperature) will be very important information. Thus, the coupling procedure proposed above is validated based on the Case 2. The temperature fluctuating frequency is $f_{re} = 100$ Hz to approximate the combustion chamber conditions, and the fluid's thermal conductivity is restored to the real physical value. Note that the time step size of this case is reduced to $10^{-5}$ s because of the thermal properties.

Figure 5 shows the temperature evolution of the TBC-fluid interface and the solid liner-TBC interface. It can be seen that the temperature fluctuation of the TBC-fluid interface is much higher than that of the solid liner-TBC interface and the former convergence is faster than the latter, but the evolution process of the two is similar in general. Figure 6 compares the interface temperature evolution of the solid liner near the fluid side with and without TBC. It can be found that without TBC, the baseline temperature of the solid liner's interface is about 805.32 K, and the fluctuation value is about 0.1 K. For the case with TBC, the baseline temperature of the solid liner's interface is about 805.12 K, and the fluctuation value is below 0.01 K, which can be ignored. It can be seen that after employing the TBC, the overall temperature of the solid liner can be effectively reduced. Moreover, TBC greatly reduces the fluctuation value of temperature in the solid liner and reduces the risk of thermal fatigue failure. This is consistent with the previous research conclusions, which preliminarily proves that the fluid-solid coupling procedure based on the hybrid cell model and the mean-fluctuation decomposition scheme can be used in the fluid-solid-solid case.

The comparison of converged interface temperature is shown in Figure 7. The performance of the different schemes is similar to Case 1. It is worth noting that at the liner-TBC interface, the fluctuation of the desynchronizing model has been overestimated by 1-2 orders of magnitude, which further reflects the superiority of the mean-fluctuation decomposition scheme in the accurate prediction of fluctuation.. The comparison of mean interface temperature is shown in Figure 8. It can be seen that the solid liner-TBC-fluid coupling procedure with mean-fluctuating decomposition can still speed up the convergence compared to the synchronizing model. Therefore, this fluid-solid-solid coupling procedure achieves desired speedup ratio and accuracy to some extent.

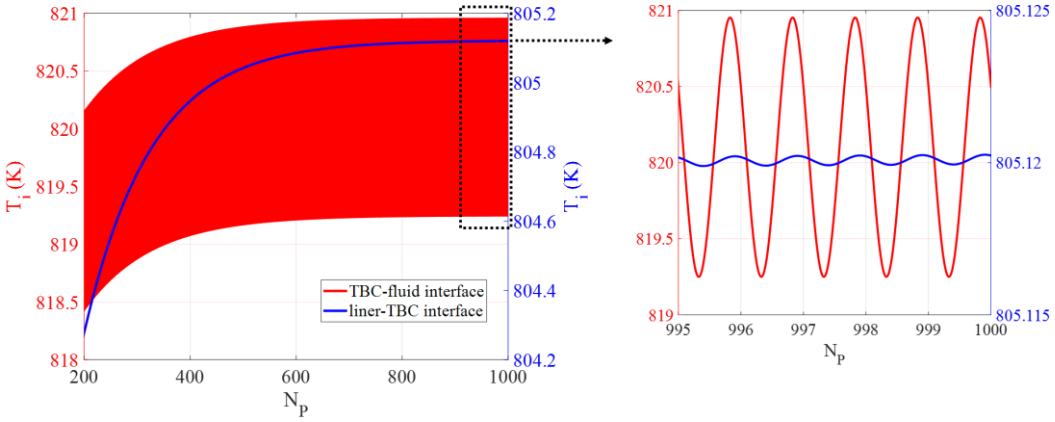


**Figure 5 Evolution of the TBC-fluid and liner-TBC interface temperature**

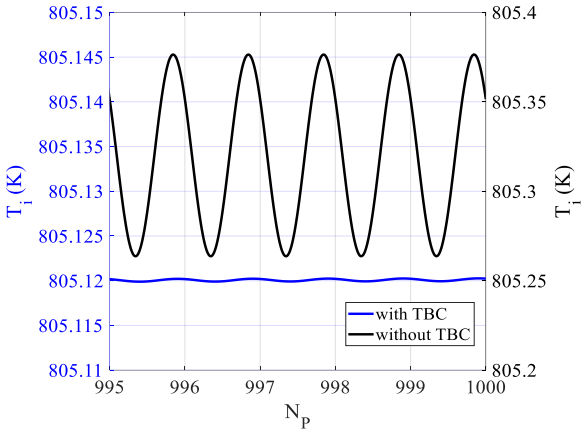


**Figure 6 Evolution of the converged liner-TBC/liner-fluid interface temperature with/without TBC**

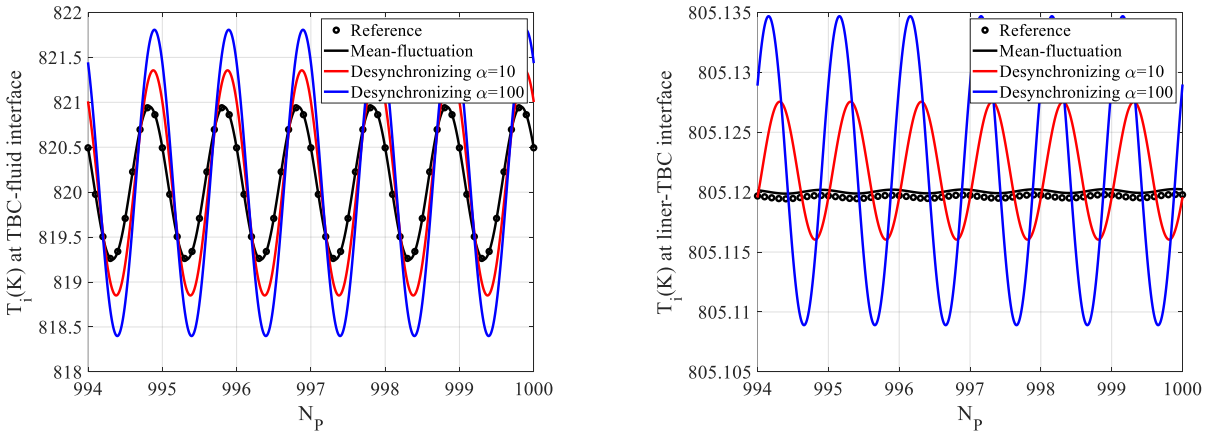


(a) TBC-fluid interface (b) liner-TBC interface

**Figure 7 Comparison of converged (a) TBC-fluid and (b) liner-TBC interface temperature evolutions using different coupling schemes**

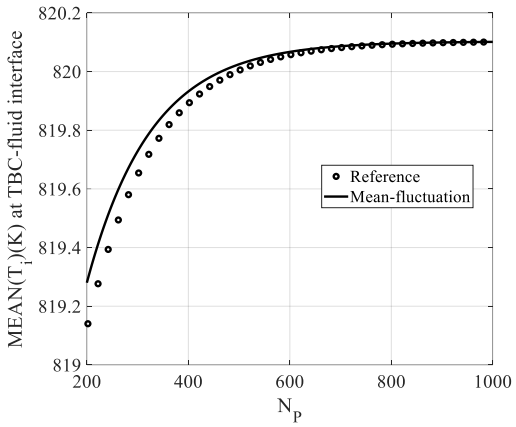


(c) TBC-fluid interface

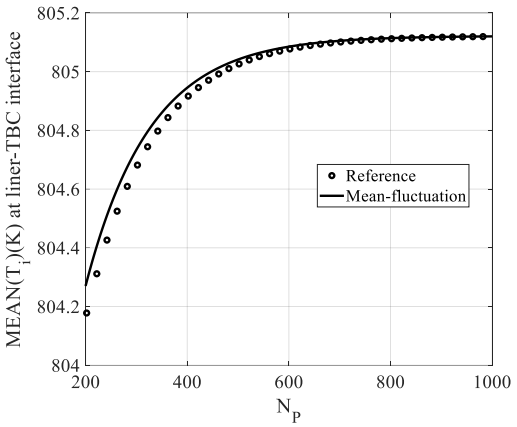


(d) liner-TBC interface

**Figure 8 Comparison of mean (a) TBC-fluid and (b) liner-TBC interface temperature evolutions using mean-fluctuation and synchronizing (reference) coupling schemes**

## CONCLUSIONS

In this study, a mean-fluctuation decomposition scheme is introduced and validated by solving the fluid-solid coupled CHT problems with inherently wide disparity of time scales. To accelerate the convergence for more complex simulation in the combustor, a fluid-solid-solid coupling procedure for solid liner-TBC-fluid system based on the hybrid cell model and mean-fluctuation decomposition scheme is proposed. Furthermore, these coupling procedures are validated in the 1-D solid liner-fluid and solid liner-TBC-fluid cases which are simplified from the real combustor conditions. In the solid liner-fluid case, although the result of desynchronizing coupling model shows considerable acceleration, the large deviations of temperature amplitudes cannot be neglected. In contrast, the mean-fluctuation decomposition scheme can accelerate the fluid-solid coupling heat transfer process about 6 times and also ensure the accuracy of the converged results. For the solid liner-TBC-fluid case, the novel fluid-solid-solid coupling procedure based on the hybrid cell model and the mean-fluctuation decomposition scheme has been tested to be effective and applicable. The results show that the overall temperature of the solid liner can be effectively reduced after employing the TBC, and also the TBC greatly reduces the temperature's fluctuation. Moreover, compared with other coupling schemes, this novel coupling procedure can ensure the prediction accuracy of fluctuation, and also achieve the desired calculation acceleration in the fluid-solid-solid coupling case.

## NOMENCLATURE

| | |
|---|---|
| $C_p$ | specific heat capacity (J/kg·K) |
| $H$ | enthalpy (J) |
| $L$ | length (mm) |
| $N$ | number of iterations |
| $t$ | time (s) |
| $T$ | temperature (K) |
| $\Delta t$ | time step (s) |
| $V$ | mesh volume ($m^3$) |
| $x, y$ | Cartesian coordinates (mm) |
| *Greeks* | |
| $\alpha$ | desynchronization factor |
| $\lambda$ | thermal conductivity ($W \cdot m^{-1} \cdot K^{-1}$) |
| $\mu$ | dynamic viscosity ($kg \cdot m^{-1} \cdot s^{-1}$) |
| $\rho$ | density ($kg/m^3$) |
| $\phi$ | heat flux (W) |

*Abbreviations*

| | |
|---|---|
| CHT | Conjugate Heat Transfer |
| DNS | Direct Numerical Simulation |
| LES | Large Eddy Simulation |
| ODE | Ordinary Differential Equation |
| TBC | Thermal Barrier Coating |

*Subscripts*

| | |
|---|---|
| $f$ | fluid domain |
| $hyb$ | hybrid |
| $i$ | fluid-solid interface |
| $n$ | temporal index |
| $opt$ | optimal |
| $P$ | period |
| $s$ | solid domain |
| $tbc$ | TBC domian |

*Superscripts*

| | |
|---|---|
| $p, q, n$ | temporal index |


## ACKNOWLEDGMENTS

The work is supported by the National Key Research and Development Program of China (No. 2021YFA0719202) and the National Natural Science Foundation of China (No. 52106048 & 52025062).


## REFERENCE


Baqué, B., Errera, M., Roos, A. and Feyel, F. (2013). Simulation of Transient Conjugate Heat Transfer Via a Temporal Multiscale Approach. *International Journal for Multiscale Computational Engineering*, 11(4), 333-345. https://doi.org/10.1615/IntJMultCompEng.2013004653.

Berger, S., Richard, S., Duchaine, F., Staffelbach, G. and Gicquel, L. (2016). On the Sensitivity of a Helicopter Combustor Wall Temperature to Convective and Radiative Thermal Loads. *Applied Thermal Engineering*, 103, 1450-1459. https://doi.org/10.1016/j.applthermaleng.2016.04.054.

Birken, P., Quint, K. J., Hartmann, S. and Meister, A. (2010). A Time-Adaptive Fluid-Structure Interaction Method for Thermal Coupling. *Computing and Visualization in Science*, 13(7), 331-340. https://doi.org/10.1007/s00791-010-0150-4.

Duchaine, F., Corpron, A., Pons, L., Moureau, V., Nicoud, F. and Poinsot, T. (2009a). Development and Assessment of a Coupled Strategy for Conjugate Heat Transfer with Large Eddy Simulation: Application to a Cooled Turbine Blade. *International Journal of Heat and Fluid Flow*, 30(6), 1129-1141. https://doi.org/10.1016/j.ijheatfluidflow.2009.07.004.

Duchaine, F., Jauré, S., Poitou, D., Quémerais, E., Staffelbach, G., Morel, T. and Gicquel, L. (2015). Analysis of High Performance Conjugate Heat Transfer with the Openpalm Coupler. *Computational Science & Discovery*, 8(1), 015003. https://doi.org/10.1088/1749-4699/8/1/015003.

Duchaine, F., Maheu, N., Moureau, V., Balarac, G. and Moreau, S. (2014). Large-Eddy Simulation and Conjugate Heat Transfer around a Low-Mach Turbine Blade. *Journal of Turbomachinery*, 136(5), 051015. https://doi.org/10.1115/1.4025165.

Duchaine, F., Mendez, S., Nicoud, F., Corpron, A., Moureau, V. and Poinsot, T. (2009b). Conjugate Heat Transfer with Large Eddy Simulation for Gas Turbine Components. *Comptes Rendus Mécanique*, 337(6), 550-561. https://doi.org/10.1016/j.crme.2009.06.005.

Errera, M. P. and Baqué, B. (2013). A Quasi‐Dynamic Procedure for Coupled Thermal Simulations. *International Journal for Numerical Methods in Fluids*, 72(11), 1183-1206. https://doi.org/10.1002/fld.3782.

Errera, M. P. and Chemin, S. (2013). Optimal Solutions of Numerical Interface Conditions in Fluid–Structure Thermal Analysis. *Journal of Computational Physics*, 245, 431-455. https://doi.org/10.1016/j.jcp.2013.03.004.

Errera, M. P., Lazareff, M., Garaud, J. D., Soubrié, T., Douta, C. and Federici, T. (2017). A Coupling Approach to Modeling Heat Transfer During a Full Transient Flight Cycle. *International Journal of Heat and Mass Transfer*, 110, 587-605. https://doi.org/10.1016/j.ijheatmasstransfer.2017.03.048.

Errera, M. P., Moretti, R., Mayeur, J., Gelain, M., Tessé, L., Lamet, J. M. and Laroche, E. (2020). A Numerical Predictive Model for Conjugate Heat Transfer with Radiation. *International Journal of Heat and Mass Transfer*, 160, 120155. https://doi.org/10.1016/j.ijheatmasstransfer.2020.120155.
Geiser, J. and Güttel, S. (2012). Coupling Methods for Heat Transfer and Heat Flow: Operator Splitting and the Parareal Algorithm. *Journal of Mathematical Analysis and Applications*, 388(2), 873-887. https://doi.org/10.1016/j.jmaa.2011.10.030.
Giles, M. B. (1997). Stability Analysis of Numerical Interface Conditions in Fluid–Structure Thermal Analysis. *International Journal for Numerical Methods in Fluids*, 25(4), 421-436. https://doi.org/10.1002/(SICI)1097-0363(19970830)25:4<421::AID-FLD557>3.0.CO;2-J.
Gimenez, G., Errera, M., Baillis, D., Smith, Y. and Pardo, F. (2016). A Coupling Numerical Methodology for Weakly Transient Conjugate Heat Transfer Problems. *International Journal of Heat and Mass Transfer*, 97, 975-989. https://doi.org/10.1016/j.ijheatmasstransfer.2016.02.037.
He, L. and Oldfield, M. L. G. (2010). Unsteady Conjugate Heat Transfer Modeling. *Journal of Turbomachinery*, 133(3), 031022. https://doi.org/10.1115/1.4001245.
Heselhaus, A. and Vogel, D. (1995). Numerical Simulation of Turbine Blade Cooling with Respect to Blade Heat Conduction and Inlet Temperature Profiles. *AIAA the 31st Joint Propulsion Conference and Exhibit*, 1995. https://doi.org/10.2514/6.1995-3041.
Jauré, S. 2012. *Methodology for Conjugate Heat Transfer Simulations Relying on Large Eddy Simulations in Massively Parallel Environments.* PhD Thesis, Institut National Polytechnique de Toulouse-INPT.
Jaure, S., Duchaine, F., Staffelbach, G. and Gicquel, L. (2013). Massively Parallel Conjugate Heat Transfer Methods Relying on Large Eddy Simulation Applied to an Aeronautical Combustor. *Computational Science & Discovery*, 6(1), 015008. https://doi.org/10.1088/1749-4699/6/1/015008.
Koren, C., Vicquelin, R. and Gicquel, O. (2017a). An Acceleration Method for Numerical Studies of Conjugate Heat Transfer with a Self-Adaptive Coupling Time Step Method: Application to a Wall-Impinging Flame. *Proceedings of the ASME Turbo Expo 2017: Power for Land, Sea, and Air*, Charlotte, North Carolina, USA, 2017. https://doi.org/10.1115/GT2017-64224.
Koren, C., Vicquelin, R. and Gicquel, O. (2017b). Self-Adaptive Coupling Frequency for Unsteady Coupled Conjugate Heat Transfer Simulations. *International Journal of Thermal Sciences*, 118, 340-354. https://doi.org/10.1016/j.ijthermalsci.2017.04.023.
Li, H. and Kassab, A. (1994). Numerical Prediction of Fluid Flow and Heat Transfer in Turbine Blades with Internal Cooling. *AIAA the 30th Joint Propulsion Conference and Exhibit*, 1994. https://doi.org/10.2514/6.1994-2933.
Lindström, J. and Nordström, J. (2010). A Stable and High-Order Accurate Conjugate Heat Transfer Problem. *Journal of Computational Physics*, 229(14), 5440–5456. https://doi.org/10.1016/j.jcp.2010.04.010.
Liu, Q., Huang, S. and He, A. (2019). Composite Ceramics Thermal Barrier Coatings of Yttria Stabilized Zirconia for Aero-Engines. *Journal of Materials Science & Technology*, 35(12), 2814-2823. https://doi.org/10.1016/j.jmst.2019.08.003.
Lv, F., Li, Q. and Fu, G. (2010). Failure Analysis of an Aero-Engine Combustor Liner. *Engineering Failure Analysis*, 17(5), 1094-1101. https://doi.org/10.1016/j.engfailanal.2010.01.003.
Song, J. B., Wang, L. S., Dong, H. and Yao, J. T. (2023). Long Lifespan Thermal Barrier Coatings Overview: Materials, Manufacturing, Failure Mechanisms, and Multiscale Structural Design. *Ceramics International*, 49(1), 1-23. https://doi.org/10.1016/j.ceramint.2022.10.222.
Verstraete, T. and Van den Braembussche, R. (2009). A Novel Method for the Computation of Conjugate Heat Transfer with Coupled Solvers. *Proceedings of International Symposium on Heat Transfer in Gas Turbine Systems*, Antalya, Turkey, 2009. https://doi.org/10.1615/ICHMT.2009.HeatTransfGasTurbSyst.570.
Zhang, J., Dai, H., Lin, J., Yuan, Y., Liu, Z., Sun, Y. and Ding, K. (2020). Cracking Analysis of an Aero-Engine Combustor. *Engineering Failure Analysis*, 115, 104640. https://doi.org/10.1016/j.engfailanal.2020.104640.